Magnetic - Nonmagnetic Substituted Spinel Ferrite $Fe_{2(1-t)}Mg_{1+t-x}Ni_xTi_tO_4$ Study Using Xfit-Koalarie Program

Dr.Abdurazak.M.Alakrmi [(1)], Afaf.S.Alzawaly [(2)] Mahmoud.M.Elakrami[(3)]
Dr.Abdusalam.M.Algamoudi [(4)]
Department of Physics[(1,2)]and Department of Computer[(3)]- Faculty of Education - Zawia University.
Department of Physics[(4)] - Faculty of Science - Aljapal Algharbi University

Abstract :

Magnetic - nonmagnetic (1+ t) $Mg^{2+} \rightarrow Mg^{2+} + Ni^{2+}$ substituted can be made in well known spinel ferrites $Fe_{2(1-t)}Mg_{1+t}Ti_tO_4$, were prepared by the conventional solid - state reaction sintering technique at 1300^0C and investigated by X-ray powder diffraction spectroscopic technique using X-ray Line Profile Fitting Program, Xfit-Koalarie, the recorded reflection planes proved that all the prepared samples have cubic single phase spinel structure which indexed to the *Fd*3*m* space group. The true lattice parameters are determined accurately using Nelson-Riley extrapolation function. The density and distance between magnetic ions for both

octahedral sites and tetrahedral sites are discussed depending on the composition parameter. The lattice parameter were found to be decrease linearly with increasing nickel concentration, thus obeying Vegard's law, this variation is assigned to the substitution process and the migration of the Fe^{+3} ions with relatively small radius (0.64Å) into the A-sites on expense of Mg^{2+} ions (0.66Å). The decrement of the hopping lengths is attributed to the substitution process and different in ionic radii which makes that magnetic ions Fe^{3+} and Ni^{+2} on B-sites and Fe^{3+} ions on A-sites become closer to each other, whereas, the density increases may be attributed to the replacement process and the influence of the difference in atomic weight of cations. all that parameters are influenced by the nickel concentration and cation distribution, thus will have an important effect on fundamental magnetic and electric properties.

Key words: *X-ray diffraction ; Xfit-Koalarie Program; spinel ferrites; precise lattice parameters;* Fe Mg Ni Ti O_4

Corresponding author: *Tel.: +218927435358; E-mail address: Razak2016a@gmail.com*
(Assist. Prof. Dr. A.M. Alakrmi [(1)])

Introduction :

The ideal spinel crystal structure is known indexed to the *Fd*3*m* space group, which based on cubic close packing arrays of anions along [111], with inter-holes of tetrahedral (A-sites) and octahedral (B-sites), the A-site is the space between four negative anions, while the space which formed by six anions is called octahedral B-site, the relative sizes holes of each geometry are usually the octahedral space is larger than the tetrahedral space and the anions with radius (r_o) are usually larger than cations with radius (r_c) giving a radius ratio less than 1.00, the largest atom that can fit into a tetrahedral hole without distorting as shown in Figure.(1) the

tetrahedron has a radius only 0.225 times the radius of the atoms that form the hole constrained by the relation $0.225 \leq r_c/r_o \leq 0.414$. If $r_c/r_o = 0.225$, the anion layers are closest-packed. whereas, the structure of having ions with radii smaller than 0.225 r_o in the tetrahedral site is unstable. When the cation radii are greater or equal to 0.414 r_o , but less than 0.732 r_o , the cations occupy the octahedral sites, if the cations are large such that $r_c \geq 0.732\ r_o$, the cation will have a cubic coordination of 8.

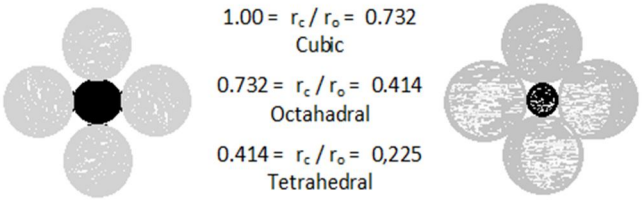

Fig.(1): *Pauling's 1st Rule - Radius Ratio* [1].

The spinel have general chemical formula (A) $[B]_2\ X_4$ where A divalent cations, B trivalent and X negative anions, the spinel oxide can be represent by the formula $(A^{2+}_{1-\delta}\ B^{3+}_{\delta})\ [A^{2+}_{\delta}\ B^{3+}_{2-\delta}]\ O^{2-}_4$. Figure.(2) shows the unit cell of normal spinel oxide AB_2O_4 contains 8 tet, 16 oct and 32 O^{2-} sites, the figure is illustrating the A and B-sites locations relative to each other and to the O^{2-} lattice, the oxygen ions reside on a face-centered-cubic lattice of a_0 /2 , while the *A*-site ions reside on the interstices of two interpenetrating fcc lattices of a_0 and the *B*-site ions reside on the interstices of four interpenetrating fcc lattices of a_0, more information are available elsewhere [2,3].

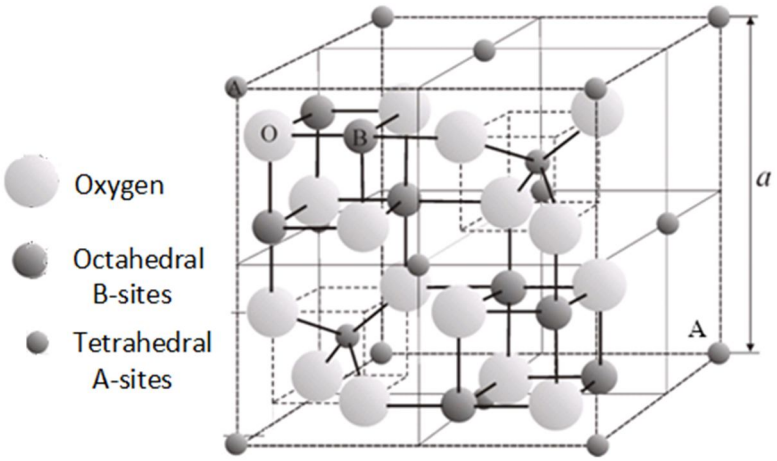

Fig.(2): *The AB_2O_4 unit cell* [3].

In general, any ions on A and B will have different sizes, as well as, the two kind of holes have different sizes, the same positive ion can be peck in these different holes of each geometry, they will differ in ionic radii which are determined by measuring the distance between adjacent nuclei, thus any change in chemical compositions (x) and replacement process, these will result in a corresponding adjustment variations of the structural parameters, such as lattice parameter (a), oxygen parameter (u) and intr-atomic spacing [2], moreover, the introduction of larger ions results in an increase of the distance between the magnetic ions which determine by lattice constant, many spinels could be explained on the basic of the correlation between the ionic radius and the lattice parameters [4,5], the larger ionic radii causes a considerable expansion of unit cell volume resulting in an increase of the lattice parameter, for examples $Mg_{1.3-x}Fe_{1.4}Zn_xTi_{0.3}O_4$ system [6] and the system $Mg_{1-x}Zn_xFe_2O_4$ [7], the increase of the lattice parameter was due to the replacement of smaller ionic radius Mg^{2+}(0.66Å) by larger ionic radius of Zn^{2+} ion (0.74Å) on the tetrahedral sites. Also in the system $Mg_{1+t}Fe_{2-2t}Ti_tO_4$ [8], the increases of

lattice constant result from migration of Mg^{2+} ions to A-sites replaced by tetra- Fe^{3+} at high temperature. On the other hand, the replacement of the larger ionic radius by the smaller causes the shrinkage of the unit cell dimensions[2,9,10], in the case of replacement cations with about equal radii, just as in the system $Ni_{1+t}\ Fe_{2-2t}\ Ti_tO_4$ [11] and in the system $Li_{0.5+0.5t}Ti_t\ Fe_{2.5-1.5t}\ O_4$ [12], this is expected on lattice parameter to be nearly independent of composition parameter, thus the cationic substitution has not affected [12] If the variation of lattice constant is quite dependence on composition parameter (x), then obeying Vegard's law [4,13]. Another important point, that is possible to investigate the influence of those parameters upon the electric and magnetic properties [7].

In fact, a little information is available in the literature regarding influence of Ni^{2+} cations on physical properties of the spinel with general formula $Fe_{0.6}\ Mg_{1.7-x}\ Ni_x\ Ti_{0.7}\ O_4$ is discussed elsewhere [14]. In the present paper we investigate in extensive details the results of x-ray diffraction spectrometer as diagnostic technique with increasing magnetic concentration (Ni^{2+}) on the expenses of diamagnetic concentration (Mg^{2+}). Also aimed to discuss that, the effects on electric and magnetic properties may be arising from the change in dimension of the magnetic and non-magnetic ions and their distributions over the two sub-lattices of the samples under investigation.

Experimental Techniques :

The proposed ferrite samples having the general chemical formula $Fe_{0.6}\ Mg_{1.7-x}\ Ni_x\ Ti_{0.7}\ O_4$, with x = 0.1, 0.15, 0.2, 0.25 and 0.3, were prepared by the conventional solid – state reaction sintering technique. The starting dry materials oxides NiO, MgO, TiO_2 and Fe_2O_3 high purity were mixed together in approximate molar ratio, the resulting mixtures were

pressed into a small pellets under the pressure of 5 tons/cm^2 and they were pre - fired treatment at 900 C^o for 18 hr, then slowly cooled to room temperature. These pellets were again followed by grinding, pressing into pellets and sintered at 1300 ^{0}C for 24 hr in air , and then slowly cooled to room temperature. X-ray powder diffraction using Cu-Ka – radiation were applied to determine the structural properties, the data were collected on computer controlled Philips Analytical X-Ray diffractometer, Type PW3710.

Results and Discussion :

The $Fe_{0.6}$ $Mg_{1.7-x}$ Ni_x $Ti_{0.7}$ O_4 Ferrite specimens in a concentration range ($0.1< x < 0.3$) at 1300 C^o were prepared for investigate their Structure properties. The starting materials oxides NiO, MgO, TiO_2 and Fe_2O_3 are shown in Table.(1).

Table.(1): *Weight of the starting oxides (in grams).*

x	Compounds	TiO_2	NiO	MgO	Fe_2O_3
0.1	$Fe_{0.6}Mg_{1.7-x}Ni_xTi_{0.7}O_4$	3.1814	0.4246	3.6676	2.7250
0.15	$Fe_{0.6}Mg_{1.7-x}Ni_xTi_{0.7}O_4$	3.1492	0.6310	3.5184	2.7012
0.2	$Fe_{0.6}Mg_{1.7-x}Ni_xTi_{0.7}O_4$	3.1190	0.8336	3.3734	2.6726
0.25	$Fe_{0.6}Mg_{1.7-x}Ni_xTi_{0.7}O_4$	3.0890	1.0320	3.2298	2.6472
0.3	$Fe_{0.6}Mg_{1.7-x}Ni_xTi_{0.7}O_4$	3.0614	1.2268	3.0892	2.6220

The x-ray powder diffraction (XRD) patterns revealed in the 15^0 – 80^0, 2θ range that samples have single cubic spinel phases belong to *Fd3m* space group. The main reflection planes are the same for all samples explained in figure.(3) as an example.

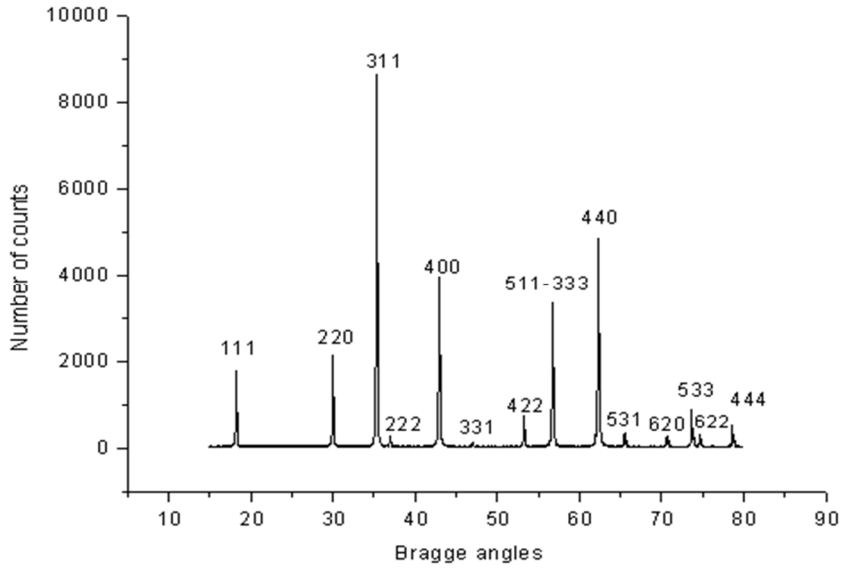

Fig.(3): *X-ray powder diffraction patterns of* $Fe_{0.6}Mg_{1.7-x}Ni_xTi_{0.7}O_4$ *Spinel ferrites*

The goodness of fit is going a good or bad value depends on actual data and type of sample, the best fit of line positions were accomplished by using x-ray Line Profile Fitting Program, Xfit-Koalarie program (Cheary and Coelho, 1996) [15], it implicitly corrected Bragg 2θ positions through the use of Pseudo Voigt (PV) profile function, to each reflection start a refinement by Select on the position of the CuKα1 peak only, providing peak positions (2θ), full width at Half-maximum (FWHM) and the relative areas under the peaks (A), the corresponding interplanar distances (d_{hkl}) have been calculated from the Bragg angle 2θ and the hkl values, thus the lattice parameters a_{hkl} from the reflection planes are given by: [16,17]

$$a_{hkl} = d_{hkl}\sqrt{h^2 + k^2 + l^2}$$

However, as fitted and calculated Structure parameters of each sample are listed in Tables 2,3,4,5 and 6.

Table.(2): *Fitted results of X-ray D from XFIT program of $Fe_{0.6}Mg_{1.6}Ni_{0.1}Ti_{0.7}O_4$ (X=0.1)*

Peak	2θ	Area	FWHM	d- space	h k l	F (Θ)	a_{hkl} (Å)
1	18.2622	218.2219	0.1078	4.85399	111	3.1247494	8.407366
2	30.0077	339.6938	0.1067	2.97546	220	1.8330166	8.415884
3	35.3347	1544.218	0.1062	2.53813	311	1.5214490	8.418053
4	36.9781	22.2295	0.1958	2.42902	222	1.4424349	8.414381
5	42.9318	777.0518	0.1057	2.10494	400	1.2035162	8.419788
6	46.9916	6.2981	0.0987	1.93211	331	1.0726898	8.421903
7	53.2396	134.0708	0.1050	1.71915	422	0.9068799	8.422122
8	56.7472	630.4146	0.1069	1.62093	511-333	0.8281797	8.422637
9	62.3053	992.7325	0.1089	1.48902	440	0.7196145	8.423171
10	65.5011	51.5926	0.1052	1.42389	531	0.6645518	8.423850
11	70.6632	47.4112	0.1166	1.33198	620	0.5848566	8.424244
12	73.6793	152.0893	0.1166	1.28473	533	0.5428248	8.424589
13	74.6718	52.0782	0.1196	1.27010	622	0.5296430	8.424903
14	78.6021	92.3123	0.1123	1.21614	444	0.4803174	8.425697

Table.(3): *Fitted results of X-ray D from XFIT program of $Fe_{0.6}Mg_{1.55}Ni_{0.15}Ti_{0.7}O_4$ (X=0.15)*

Peak	**2θ**	**Area**	**FWHM**	**d- space**	**h k l**	**F (Θ)**	**a_{hkl} (Å)**
1	18.2073	188.3928	0.1147	4.86850	111	3.13457	8.432502
2	29.9582	282.9018	0.1210	2.98026	220	1.83640	8.429471
3	35.2870	1357.076	0.1138	2.54146	311	1.52384	8.429069
4	36.9192	19.9139	0.1676	2.43276	222	1.44515	8.427337

Peak	2θ	Area	FWHM	d- space	h k l	F (Θ)	a_{hkl} (Å)
5	42.8897	655.3138	0.1176	2.10691	400	1.20499	8.427663
6	46.9731	6.3928	0.1614	1.93283	331	1.07323	8.425031
7	53.2104	122.1378	0.1043	1.72003	422	0.90757	8.426406
8	56.7157	597.2019	0.1040	1.62176	511-333	0.82884	8.426927
9	62.2773	930.0466	0.1021	1.48962	440	0.72011	8.426578
10	65.4783	51.8961	0.1031	1.42433	531	0.66492	8.426457
11	70.6406	44.6191	0.1019	1.33236	620	0.58518	8.426588
12	73.6542	148.3939	0.1071	1.28511	533	0.54316	8.427053
13	74.6532	48.9204	0.1061	1.27037	622	0.52988	8.426697
14	78.5911	84.0584	0.1016	1.21628	444	0.48044	8.426685

Table.(4): *Fitted results of X-ray D from XFIT program of $Fe_{0.6}Mg_{1.5}Ni_{0.2}Ti_{0.7}O_4$ (X=0.2)*

Peak	Th2	Area	FWHM	d- spac	h k l	F (Θ)	a_{hkl} (Å)
1	18.2690	223.3621	0.1145	4.85220	111	3.1235364	8.4042639
2	30.0196	331.6524	0.1202	2.97431	220	1.8322044	8.4126249
3	35.3505	1575.4968	0.1157	2.53704	311	1.5206567	8.4144106
4	36.9869	32.6824	0.0867	2.42846	222	1.4420294	8.4124498
5	42.9502	735.1581	0.1109	2.10408	400	1.2028726	8.4163522
6	47.0194	8.3604	0.1225	1.93103	331	1.0718648	8.4172060
7	53.2703	139.3889	0.1084	1.71824	422	0.9061513	8.4176228
8	56.7791	668.0565	0.1033	1.62010	511-333	0.8275035	8.4182991
9	62.3432	1019.3373	0.1065	1.48820	440	0.7189327	8.4185662

Peak	Th2	Area	FWHM	d- spac	h k l	F (Θ)	a_{hkl} (Å)
10	65.5414	55.9150	0.1098	1.42311	531	0.6638874	8.4192481
11	70.7113	49.1737	0.1062	1.33120	620	0.5841618	8.4192596
12	73.7250	165.3328	0.1104	1.28405	533	0.5422110	8.4201077
13	74.7205	53.6807	0.1129	1.26939	622	0.5290041	8.4202132
14	78.6593	87.7586	0.1062	1.21540	444	0.4796316	8.4205631

Table.(5): *Fitted results of X-ray D from XFIT program of* $Fe_{0.6}Mg_{1.45}Ni_{0.25}Ti_{0.7}O_4(X=0.25)$

Peak	Th2	Area	FWHM	d- spac	h k l	F (Θ)	a_{hkl} (Å)
1	18.2502	261.8446	0.1126	4.85716	111	3.1268921	8.4128479
2	30.0082	346.4266	0.0925	2.97541	220	1.8329825	8.4157474
3	35.3420	1566.124	0.0966	2.53763	311	1.5210828	8.4163697
4	36.9688	37.8322	0.1088	2.42961	222	1.4428636	8.4164245
5	42.9444	732.6084	0.1015	2.10435	400	1.2030754	8.4174352
6	47.0212	10.4193	0.0947	1.93096	331	1.0718114	8.4169021
7	53.2693	141.0390	0.0830	1.71826	422	0.9061750	8.4177693
8	56.7803	654.1853	0.0779	1.62007	511-333	0.8274781	8.4181360
9	62.3441	937.0944	0.0830	1.48818	440	0.7189165	8.4184569
10	65.5450	54.8601	0.0836	1.42304	531	0.6638281	8.4188373
11	70.7104	48.8699	0.0922	1.33121	620	0.5841748	8.4193528
12	73.7317	181.4026	0.0836	1.28395	533	0.5421211	8.4194512
13	74.7265	48.4542	0.0862	1.26930	622	0.5289254	8.4196358
14	78.6679	91.6390	0.0760	1.21529	444	0.4795285	8.4197919

Table.(6): *Fitted results of X-ray D from XFIT program of* $Fe_{0.6}Mg_{1.4}Ni_{0.3}Ti_{0.7}O_4$ *(x=0.3)*

Peak	Th2	Area	FWHM	d- spac	h k l	F (Θ)	a_{hkl} (Å)
1	18.2580	227.8375	0.1423	4.85510	111	3.1254990	8.4092843
2	30.0185	324.1242	0.1341	2.97441	220	1.8322794	8.4129261
3	35.3526	1587.043	0.1298	2.53689	311	1.5205514	8.4139267
4	36.9844	38.4704	0.1581	2.42862	222	1.4421446	8.4129985
5	42.9605	767.4373	0.1209	2.10360	400	1.2025126	8.4144297
6	47.0336	14.5498	0.1251	1.93048	331	1.0714437	8.4148090
7	53.2885	139.8421	0.1053	1.71769	422	0.9057197	8.4149581
8	56.8000	659.7251	0.1102	1.61955	511-333	0.8270609	8.4154593
9	62.3668	987.7061	0.1093	1.48769	440	0.7185085	8.4157013
10	65.5678	55.5521	0.1076	1.42260	531	0.6634526	8.4162363
11	70.7343	46.9026	0.1171	1.33082	620	0.5838299	8.4168786
12	73.7575	166.5868	0.1086	1.28356	533	0.5417749	8.4169243
13	74.7617	58.3593	0.1013	1.26879	622	0.5284641	8.4162503
14	78.6971	92.1407	0.1036	1.21491	444	0.4791788	8.4171748

To determine the precise lattice parameters as accurately as possible of materials with considering the sources of error described elsewhere [16], we refined the lattice parameter by using the Nelson-Riley procedure, the corrected values of lattice parameters are accurately determined by plotting the values of a_{hkl} for each peak against the Nelson-Riley function $F(\theta)$ were given in the tables above and defined by: [16,18]

$$F(\theta) = \frac{1}{2}\left[\frac{\cos^2\theta}{\sin\theta} + \frac{\cos^2\theta}{\theta}\right]$$

A straight line $a_{hkl} = a_0 + CF(\theta)$ is fitted to the points and extrapolation to θ = 90°. Yields $a_{hkl} = a_0$. The fitting results for the different samples are shown in Figures 4,5,6,7 and 8.

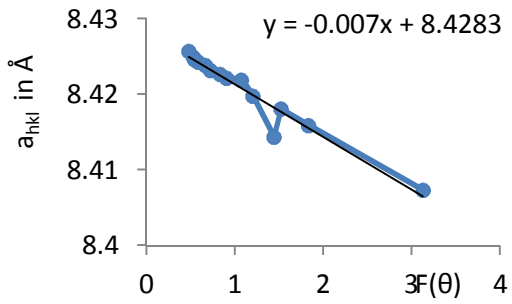

Fig.(4): *The refinement for the lattice parameter of the sample with x = 0.1.*

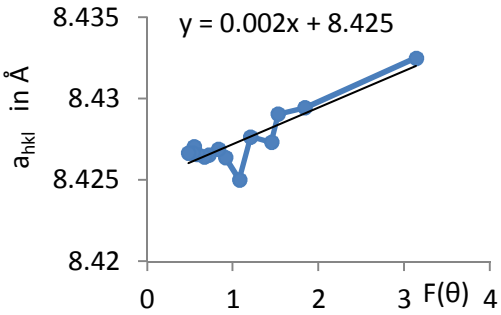

Fig.(5): *The refinement for the lattice parameter of the ample with x = 0.15*

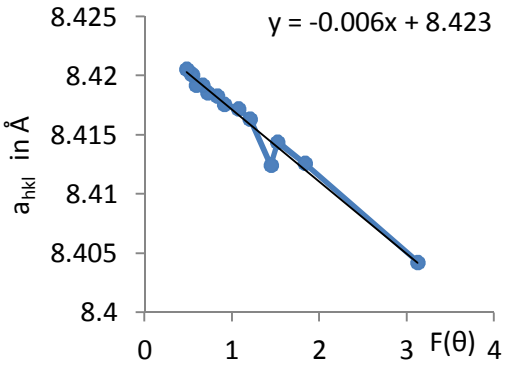

Fig.(6): *The refinement for the lattice parameter of the sample with x = 0.2*

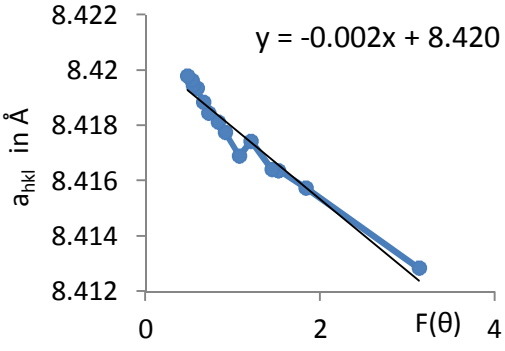

Fig.(7): *The refinement for the lattice parameter of the sample with x = 0.25*

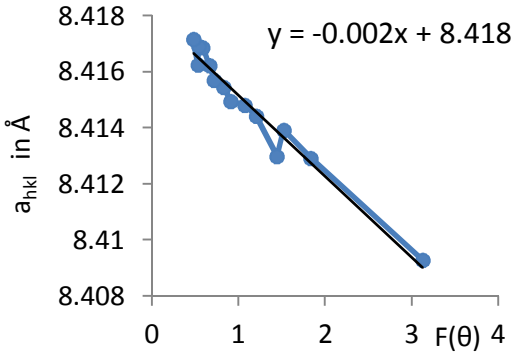

Fig.(8): *The refinement for the lattice parameter of the sample with x = 0.3*

The variation refined values of the lattice parameter as a function of composition parameter x (Ni-content) are given in Table.(7) and it is represented graphically in figure.(9), it is clearly shown that the lattice parameter exhibits a linear dependence with the composition parameter x, showing to obey Vegard's law.

Table.(7): *The calculated x-ray parameters of of $Fe_{0.6}Mg_{1.7-x}Ni_xTi_{0.7}O_4$ samples; the true lattice parameter, density and molecular weight*

x-ray parameters	samples				
Composition parameter (x)	0.1	0.15	0.2	0.25	0.3
True lattice parameter a_o in Å	8.428	8.425	8.423	8.420	8.418
Density D_x in g/cm^3	0.0390	0.0394	0.0398	0.0402	0.0407
Molecular weight M in g/mol	175.80	177.52	179.24	180.96	182.68

Starting from the basic system $Mg_{1+x}Fe_{2(1-x)}Ti_xO_4$ [8], where Mg^{2+} ions with large radius (0.66Å) are substituted to replace Fe^{3+} ions (0.64Å) on the A-sites, the replacement takes place by the movement of Fe^{3+} ions from A-sites to B-sites, this movement gave the reason of lattice parameter to increases noticeably with increase x. This is also observed in the systems $Mg_{1.3-x}Fe_{1.4}Zn_xTi_{0.3}O_4$ by *De Grave et al in 1980* [6] and $Mg_{1-x}Zn_xFe_2O_4$ by *Mazen et al in 2003* [7], the increase of the lattice parameter was due to the replacement of Mg^{2+} with a relatively small radius (0.66Å) by the larger Zn^{2+} ion (0.74Å) on the tetrahedral sites. A similar strong increase is found by replacing tetrahedral Fe^{3+} by Mg^{2+} in a $(Ni,Mg,Fe,Cr)O_4$ spinel system was reported by *Gismelseed et al., 2008* [19]. It is worthwhile to note that several studies revealed the existence of Mg^{2+} and Fe^{3+} ions on both A- and B-sites and the Ti^{4+} ions suggested occupy only B-sites, while, a stronger preference site for the Ni^{2+} ions is the B-sites. However, in our system, figure.(9) clearly shows that the lattice parameter gradually tends to decrease with increase Ni^{2+} content x, this variation may be illogical attributed to the difference in ionic radius of Ni^{2+} (0.69 Å) which is large and increases on the expenses of Mg concentration of radius (0.66 Å) on the tetrahedral sites. As a result of the replacement process which takes place by continuously migrate of Fe^{3+} ions from B-site to the A-site on the

expenses of Mg^{2+} with increasing the Ni^{2+} content, since Fe^{3+} ions on the A-sites exhibit a smaller ionic radius (0.64Å) and at the same time prevents the existence of Mg^{2+} ion on the A-sites due to stronger covalent bonding of Fe^{3+}, this movement and the smaller amount of Mg^{2+} in the small tetrahedral intersites gives the reason of the shift in figure.(9) to the lower value in the lattice parameter. The reduction of the lattice parameter means that the tetrahedral sites are shrinkage by an equal displacement of the 4 oxygen ions, at the same time the oxygen ions connected with the octahedral sites move in such a way as to expanded the size of the octahedral site by the same amount as the tetrahedral site shrink, similar behavior were observed in some spinel compounds [4,7,10].

Table.(7) also involve the variation of density D_x with Ni^{2+} content which is represented graphically in figure.(10), this parameter was calculated from x-ray using the formula: [5]

$$D_x = \frac{8M}{Na_o^3}$$

where M is the molecular weight , N Avogadro's number and a_o the true lattice parameter.

Figure.(10) shows that density increases with increasing Ni content, this is reflected in the enlargement in mass overtakes and decrease in volume of the unit cell, this increment of D_x may be attributed to the replacement process between the lighter atomic weight of Mg^{2+} ion (24.305) by the heavier as compared to that of Ni^{2+} ion (58.6934) on B-sites and continuously migrate of Fe^{3+} ion (55.847) to A- sites.

In the proposed system, we can suggest that, the increase of the Ni content will increases the tendency structure of these compounds to be inverse spinel, because of the size and the valiancy of the cations, in usually normal structure have tendency to larger cell edge [10].

The bond length is Known as the distance between the centers of adjacent atoms. So, the introduction of larger ions results in an increase of the distance between the magnetic ions, this can be investigated with XRD (Bragg's Law). The distance between magnetic ions L in both A- sites and B- site can be given by: [4,5].

$$L_{A-A} = \frac{1}{4}\, a\sqrt{2}\,, \qquad L_{B-B} = \frac{1}{4}\, a\sqrt{3}\,, \quad L_{A-B} = \frac{1}{8}\, a\sqrt{11}$$

Numerical data are listed in Table.(8). Figures.(11,12 and 13) are showing the relation between hopping length for octahedral and tetrahedral sites as a function of Ni-content (x).

***Table.(8)*:** *The calculated distance between magnetic ions L_{A-A}, L_{B-B} and L_{A-B} of $Fe_{0.6}Mg_{1.7-x}Ni_xTi_{0.7}O_4$ samples.*

hopping lengths in Å	**Ni - content (x)**				
	0.1	**0.15**	**0.2**	**0.25**	**0.3**
Tet-Tet cation (L_{A-A})	3.6495	3.6482	3.6473	3.6464	3.6451
Octa-Octa cation (L_{B-B})	2.9798	2.9787	2.9780	2.9773	2.9762
Tet-Octa cation (L_{A-B})	3.4941	3.4929	3.4920	3.4912	3.4899

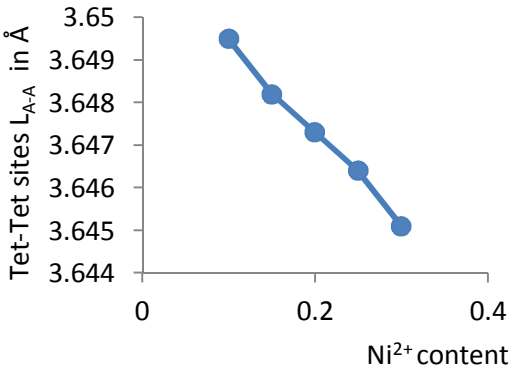

Fig.(11): *Variation of distance between magnetic ions L_{A-A} in Å as a function of x*

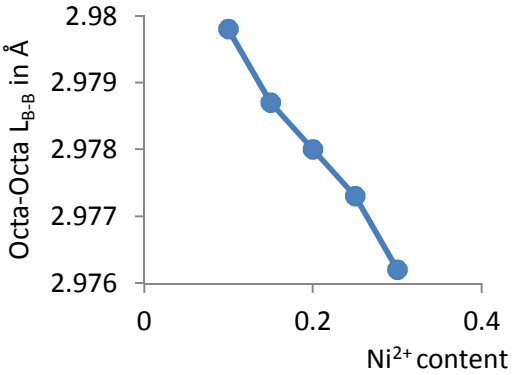

Fig.(12): *Variation of distance between magnetic ions L_{B-B} in Å as a function of x*

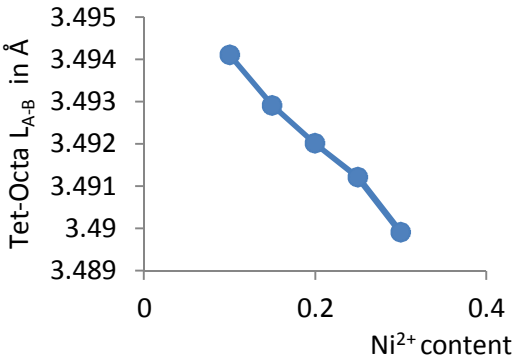

Fig.(13): *Variation of distance between magnetic ions L_{A-B} in Å as a function of x*

It is clearly that distance between magnetic ions decrease with increasing x, this is attributed to the substitution process and also may be explained on the basic of the larger radius of Ni^{+2} (0.69 Å) than that of Fe^{3+} (0.64 Å) on B-sites, which makes that magnetic ions approach or become closer to each other and decrease the hopping length L_{B-B} between them, while, the decrement of the hopping length of the tetrahedral L_{A-A} may be

attributed to the relative value of the occupancy of both smaller magnetic cations Fe^{3+} and diamagnetic Mg^{2+} in the tetrahedral site, a little amount of Mg^{2+} in the small tetrahedral interstices makes the Fe^{3+}ions become closer to each other and gives the reason of the shift in Figures.11 and 13 to the lower value in the L_{A-A} and L_{A-B} distances.

Another interesting properties are that the magnetic properties, the effects on magnetic ordering arising from the size and shape of the magnetic clusters which direct effect by a change in dimension of the non-magnetic and magnetic ions and their distributions over the two sublattices of a spinel system. Finely, the dependence on the inter-atomic distance and distributions of the magnetic atoms among two sublattices can be understood on the basis of the inter-sublattice superexchange interaction j_{A-B} between A-B and intra-sublattice superexchange interactions j_{A-A} and j_{B-B} within A-A and B-B sublattices. In order to study this influence and to obtain complete a picture of view, another powerful technique should be used, one can be confirming by Mossbauer technique.

Conclusion :

- X-ray diffraction analyses reveal a single phase spinel structure for all the samples, thus all proposed samples have been synthesized successfully.
- The corrected values of lattice parameters are accurately determined by using the Nelson-Riley extrapolation function, The lattice parameter decreases linearly with increasing nickel content may be attributed to migrate of Fe^{3+} with small ionic radius (0.64Å) from B-site to the A-site on the expenses of $Mg^{2+}$of radius (0.66 Å) and Ni^{2+} exclusively occupied B-sites only.

- The increase in the nickel content forced the structure of these samples to be inverse spinel.
- The heavier ion (larger atomic weight) bring about increment of density D_x,
- The magnetic order in spinel oxides may be investigated with XRD (Bragg's Law), it is strongly dependent on the competition between various superexchange interactions, these types of interactions in such a structure are very sensitive to the arrangement of cations over the two sublattices of a spinel system and the distance between them.

References :

[1] Linus Pauling , J. Amer. Chem. Soc. , J. Amer. Chem. Soc,51. 1010 (1929)

[2] Hugh ST, C. O'neilli and Alexandranavrots, American Mineralogist, Volume 68, pages 181-194, 1983

[3] A. M. E. Alakrmi. (2009), PhD thesis in Sciences: Physics, Ghent University.

[4] Mohamed Amer, Samy Ata-Allah, Talaat Meaz, Saad Aboul-Enein, Mohamed Abd-Elhamid, Turk J Phys 29 (2005) , 163 – 177.

[5] V.B. Kawade, G.K. Bichile, K.M. Jadhav, Materials Letters 42 (2000) 33–37

[6] E. De Grave, D. Chambaere and G. Robbecht, Phys. Stat. Sol (a) 59, (1980), 581.

[7] S. A. Mazen, S. F. Mansour, and H. M. Zaki Cryst. Res. Technol. 38, No. 6, (2003) 471 – 478*

[8] E. De Grave, J. De Sitter and R. Vandenberghe Appl. Phys. 5, (1975) 117.

[9] H. Mohan, I.A. Shaikh, R.G. Kulkarni, Physica B 217 (19961 292-298

[10] I.S. Ahmed Farag, M.A. Ahmed, S.M. Hammad, A.M. Moustafa Egypt. J. Sol., Vol. (24), No. (2), (2001)

[11] G. Blasse, Philips Res Repts suppl N3. (1964)

[12] A. A. Yousift, M. E. Elzaint, S. A. Mazent, H. H. Sutherlandt, M. H. Abdalla and S. F. Masour, Phys.: Condens. Matter 6 (1994) 5717-5724

[13] C.G. Whinfrey, D.W. Eckort, A. Tauber, J. Am. Chem. Soc. 82(1960)

[14] A. M. Alakrmi, R. E. Vandenberghe, E. De Grave, Journal of Magnetism and Magnetic Materials 321 (2009) 2365–2372

[15] R. W. Cheary and A. A. Coelho, (1996). Programs XFIT and FOURYA, deposited in CCP14 Powder Diffraction Library, Engineering and Physical Sciences Research Council, Daresbury Laboratory, Warrington, England.

(http://www.ccp14.ac.uk/tutorial/xfit-95/xfit.htm)

[16] H. P. Klug and L. E . Alexander, X-ray Diffraction Procedures, Second Edition 1974

[17] V. K. Pecharsky and P. Y. ZAVALIJ, Fundamentals of Powder Diffraction and Structural Characterization of Materials (2003)

[18] J. B. Nelson, D. P. Riley, Prot, Phys, Soe, (1945), 57, 160

[19] A. M. Gismelseed, H. Widatallah, A. D. Al-Raswas, L. Al-Omari, M. Elzain, and A. Youssif, Hyperfine Interact 184, (2008)105.